Water Air Soil Pollut (2017) 228:42
DOI 10.1007/s11270-016-3223-2

Benzalkonium Chloride Surface Adsorption and Release by Two Montmorillonites and Their Modified Organomontmorillonites

Federico M. Flores · Elsa López Loveira · Florencia Yarza · Roberto Candal · Rosa M. Torres Sánchez

Received: 26 August 2016 / Accepted: 14 December 2016

Abstract Benzalkonium chloride (BAC) loaded to montmorillonites (Mt) or organomontmorillonites (OMt) generates a functional material that can be incorporated to several systems (polymers, paints, etc) as a controlled release bactericide. Understanding the BAC adsorption sites on these adsorbents is of high importance to clarify their adsorption/desorption characteristics in aqueous media or other solvents. In this work, a thorough study about the adsorption/desorption properties of Mt and OMt with regards to BAC is presented, in order to evaluate further BAC release with the consequent aquatic environment contamination. In this work, the BAC adsorption on two different sites is demonstrated: the interlayer space and the external surface. Depending on BAC concentration in water, sorption of BAC at Mt occurred in two steps. At adsorbed amount <0.5 mmol g^{-1}, there was an Mt interlayer expansion of 0.49 nm with no change of the external charge. At adsorbed amount >0.5 mmol g^{-1}, there was a new interlayer expansion attaining 0.75 nm and the external charge shifted to positive value. In the case of OMt, the introduction of BAC produced changes in the interlayer structure and in the external surface charge. BAC desorption was strongly dependent on the type of Mt or OMt and extraction solvent, knowledge of which will allow its safe use in environmental friendly technological applications.

Keywords Montmorillonite · Organomontmorillonite · Benzalkonium chloride · Adsorption · Desorption

1 Introduction

Benzalkonium chloride (BAC), alkylbenzyldimethylam monium chloride, is a cationic surfactant with bactericide and fungicide properties, with relatively low toxicity to human beings, but hardly to degrade (Pérez et al. 2009). it is used as active ingredient in pharmaceutical and cosmetic formulations, disinfection of public health areas, cleaning of food and feed areas as well as wood preservatives (EPA and Environmental Protection 2006; Gromaire et al. 2015). As consequence of this wide range of applications (only for biocidal applications in Switzerland attains 90 tn annually; Buser and Morf 2009), BAC was detected in the aquatic environment at different concentrations, ranging from 20 to 300 μg/L in municipal wastewater (Ferrer and Furlong 2001; Zhang et al. 2015), generating an important environmental

Electronic supplementary material The online version of this article (doi:10.1007/s11270-016-3223-2) contains supplementary material, which is available to authorized users.

F. M. Flores · F. Yarza · R. M. T. Sánchez (✉)
CETMIC (Centro de Tecnología de Recursos Minerales y Cerámica) CONICET-CCT La Plata- CICBA, Camino Centenario y 506 (B1897ZCA), M. B. Gonnet, Buenos Aires, Argentina
e-mail: rosats@cetmic.unlp.edu.ar

R. M. T. Sánchez
e-mail: rosa.torres@gmail.com

E. L. Loveira · R. Candal
Instituto de Investigación en Ingeniería Ambiental and Escuela de Ciencia y Tecnología, CONICET, Universidad Nacional de General San Martín, 25 de mayo y Francia, San Martín, Buenos Aires, Argentina

Published online: 28 December 2016

concern (Zanini et al. 2013), particularly to aquatic plants (Walker and Evans 1978; Pérez et al. 2009).

Besides, the search for new active materials for the plastics and paint industries with bactericide properties had found some success with the use of metallic nanoparticles (Krishnamoorthy et al. 2014; Bellotti et al. 2015) or cationic polymers with quaternary amines (Mukherjee et al. 2008; Hoque et al. 2015). In both cases, the action of water can lead to desorption of the bactericide from the material where it is retained, providing new pollution to the aquatic environment and high production costs when wastewater treatment is applied.

Montmorillonites (Mt), due to its great adsorptive capacity, negative surface charge, and low cost, are attractive to be used as adsorbent of cationic surfactants (Tahani et al. 1999; Lagaly et al. 2006). Some cationic surfactants develop bactericide properties (Zanini et al. 2013; Özdemir et al. 2013; Bianchi et al. 2013) and have been proven effective to transfer this property to, i.e., low density polyethylene (LDPE) polymer (Savas and Hancer 2015).

A promisory functional material may be produced by the combination of BAC with Mt. Mt if used as support for BAC could locate it in both the interlayer and external surface, as happened with quaternary ammonium compounds (QAC; Bianchi et al. 2013), generating a system that can hold or release very little amount of BAC to the medium. The incorporation of this system to other material as paints, plastics, etc, would provide them antibacterial activity, diminishing the uncontrolled leaching of BAC to the environment and extending the product shelf life.

It was reported that when Mt was used as BAC adsorbent, the adsorption capacity exceeds the values of its cation exchange capacity (CEC) (Kwolek et al. 2003; Khalil 2013). This behavior was explained by Tahani et al. (1999) and further by Zanini et al. (2013) by a two-step adsorption process: at low BAC concentration the cationic exchange mechanism with high affinity constant was the main adsorption mechanism, while at high BAC concentration, with a low affinity constant, the adsorption is mainly driven by lateral interactions between surfactant molecules. These two adsorption steps could be assigned to two different surface sites, as was evidenced by the fungicide benzimidazole adsorption in Mt (Torres Sánchez et al. 2011), having each site different bond strength, and which completion was attained as the concentration of adsorbate in solution increases. The first behavior, characterized by a high affinity constant, can also be responsible for the negligible loss of surfactant when Mt loading amounts of cationic surfactant are less than the CEC (Hoque et al. 2015).

The adsorption of QAC in Mt generated the named organoclays, to which an adsorption enhancement of some organic contaminants was found by increasing the number of nonpolar sites (Gamba et al. 2015). The adsorption of hydrophobic organic contaminants on organoclays is mainly leading by a partitioning mechanism (Sheng et al. 1996) that drive it to different results depending of the organic contaminants or QAC used to attain the organoclay (Xu et al. 2011) and could help to a fast desorption of the organic contaminant involved.

The choice of solvents used to evaluate the BAC desorption was based in their industrial use mainly in paint industry and also to the generation of different modifications of the Mt interlayer. Particularly, water can increase the mobility of small quaternary ammonium ions over the surface (Gast and Mortland 1971), alcohol (EtOH) acts as a polar activators to the interlayer expansion process (Jones 1983) and could modify the surfactant arrangements in organoclay, and sodium dodecyl sulfate (SDS) is the most typical anionic surfactant used to provide strong electrostatic interactions with oppositely charged head groups of cationic surfactants.

The objective of this work was to study the adsorption capacity of BAC in two raw Mt and their organomontmorillonite (OMt) products and to analyze structural modifications and surface charge of the products with BAC by X-ray diffraction (XRD) and zeta potential (ζ) determinations, respectively. Both techniques were used to determine the BAC adsorption on interlayer or inner and external or outer surface sites. Also the release of BAC from both surface sites of the adsorbents was studied using different solvents (water, ethanol, and the anionic surfactant sodium dodecyl sulfate) in order to assess their further use in technological applications that remain green.

2 Experimental

2.1 Materials

Montmorillonite collected from Lago Pellegrini deposit (Rio Negro, North Patagonia, Argentine) was provided by Castiglioni Pes y Cia., used as received, and named M_{Cas}. The chemical formula was $[(Si_{3.89}\ Al_{0.11})\ (Al_{1.43}$

$Fe_{0.26}$ $Mg_{0.30}$)] $M^{+}_{0.41}$ (Magnoli et al. 2008) and CEC was 0.825 mmol g^{-1} clay [19]. A fraction of Mt was modified with octadecyltrimethyl-ammonium (ODTMA) bromide through ion exchange reaction at 100% CEC, following the method used previously (Gamba et al. 2015) and denoted as M_{Cas}-C18. The solid product was washed by centrifugation to free it from bromide anions ($AgNO_3$ test), dried at 80 °C, and ground in agate mortar. The QAC loading in M_{Cas}-C18 sample was 86% CEC, determined on Mt basis and by carbon analyses performed using elemental analyzer EMIA 320 V2 AC, HORIBA Jobin Yvon. The average values from three parallel measurements performed for each sample were used.

Other raw Mt, named M_{Cloi} (Cloisite-Na), and its organic modified-Mt referred as M_{Cloi}-30B (Cloisite-30B) were purchased to Southern Clay Products. The chemical formula of M_{Cloi} sample was [$(Si_{3.97}Al_{0.03})$ $(Al_{1.56}$ $Fe_{0.22}$ $Mg_{0.22})$] $M^{+}_{0.25}$ (Botana et al. 2010) and CEC was 0.926 mmol g^{-1} clay (reported by suppliers). Figure 1 showed the chemical structure of the quaternary ammonium ion in 30B with 18 carbons alkyl chain (the supplier indicated it is a mixture of ~65% C18, ~30% C16, and ~5% C14). The quaternary ammonium ion loading in M_{Cloi}-30B sample was 100% CEC (reported by suppliers). In order to eliminate the chloride counterion of M_{Cloi}-30B sample, same washing procedure as indicated for M_{Cas}-C18 sample was followed.

ODTMA bromide was purchased to Sigma Aldrich Co., purity 98%, low solubility in water, and used as received. The molecular weight (MW) of ODTMA bromide is 392.5 g mol^{-1} and critic micelle concentrations (CMC) was 0.3 mM (Rosen 1989).

Commercial benzalkonium chloride (BAC) provided by Sigma (Sigma Ultra B6295) was used in adsorption experiments and as calibration standard, respectively. The BAC product is a mixture of homologues with alkyl chains of different length being C12 the most important homologue.

BAC solutions were prepared with deionized water at pH 6.5 (Apema Osmoion, resistivity = 18 MΩ cm). The CMC values were 3.8 mM for BAC-12 and 1.18 mM for BAC-14 (Zanini et al. 2013). Figure 2 showed the chemical structure and dimensions of BAC-12, calculated using geometry optimization tools (Hyperchem software v 7.0).

SDS with a purity of 98% was provided by Cicarelli lab., with MW = 288.38 g mol^{-1} and CMC = 8 mM (Khan and Shah 2008). Ethanol 99.5% p.a. anhydrous was acquired at Sigma Aldrich.

Adsorption of BAC on M_{Cas}, M_{Cloi}, M_{Cloi}-30B, and M_{Cas}-C18 samples was performed on 1 g clay L^{-1} suspensions, equilibrated at pH 6.5, and using a BAC initial concentration (C_0) ranging from 0.01 to 1.50 mM. The BAC stock solution was 14.7 mM.

Kinetics studies performed by other authors for BAC adsorption at pH 6.5, on similar Mt, indicated that adsorption did not change from 30 min to 17 h (Zanini et al. 2013). The suspensions were shaken and equilibrated for 24 h at room temperature and solids were separated from the supernatant solutions by centrifugation at 15,000 rpm. The solids obtained were stored in desiccators over silica gel, at room temperature, for further analysis and labeled, e.g., as BAC-M_{Cas}, BAC-M_{Cloi}, etc. The amount of BAC present in the supernatant was measured by high performance liquid chromatography (HPLC) coupled with UV-visible detection by HPLC ($\lambda = 208$ nm) using a Shimadzu HPLC with a C18 column (4.6 mm × 150 mm, 4.6 μm). The mobile phase was acetonitrile (70%) and 0.0075 mM sodium phosphate buffer at pH 3 (30%) flowing at 1 mL min^{-1}. The linear range of BAC concentrations was within 0.001–2.000 mmol L^{-1} ($R^2 = 0.999$). The amounts of BAC retained by the solids were determined as the difference between initial concentration (C_0) and that of the supernatant in equilibrium (C_{eq}).

In order to compare adsorption isotherms for all samples, the experimental points obtained were adjusted by several models as Langmuir, Freundlich, and Sips. Langmuir model presented the best fitting and consequently was chosen for the analysis.

Linearized form of the Langmuir isotherm was chosen to determine the corresponding parameters (Eq. 1).

$$\frac{C_{eq}}{q_{ad}} = \frac{1}{k_L Q_{max}} + \frac{C_{eq}}{Q_{max}} \quad (1)$$

where C_{eq} is the BAC equilibrium concentration (mM), q_{ad} and Q_{max} are a BAC equilibrium and maximum amount adsorbed (mmol g^{-1}), respectively, and k_L is Langmuir adsorption constant.

Also the root mean square error (RMSE) was calculate to evaluate the goodness-of-fit, according to Eq. 2:

$$\mathrm{RMSE} = \sqrt{\frac{1}{N-2}\sum_{i=1}^{N}\left(q_{ad}^{exp} - q_{ad}^{calc}\right)^2} \quad (2)$$

where superscripts exp and calc indicate the experimental and the calculated values obtain from the fit, respectively, and N is the number of measurements.

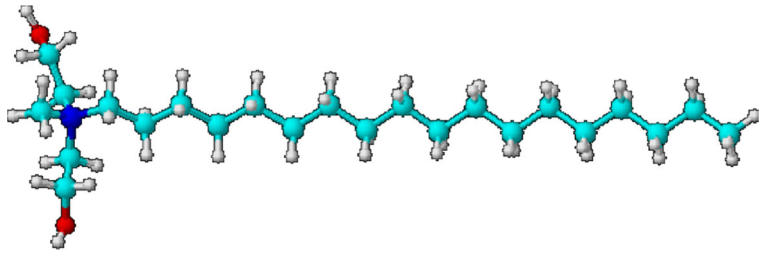

Fig. 1 Quaternary alkylammonium cation indicated as C30B

Desorption analysis were performed in triplicate on 20 mg/20 mL dispersions of BAC-M_{Cas}, BAC-M_{Cloi}, BAC-M_{Cloi}-30B, and BAC-M_{Cas}-C18 samples with maximum BAC adsorption, at water, acid, basic, ethanol 96%, or SDS 5% *w/v*. For acid or basic media, the BAC adsorbed samples were equilibrated at pH = 3.0 or pH = 11 during 1 h, by adding drops of HCl or KOH concentrated solutions. Solids were separated from the supernatant solutions by centrifugation at 15,000 rpm and supernatants were collected to determine the concentration of the desorbed BAC.

In order to attain the structure and surface electric charge modification produced by SDS or EtOH, samples of all the adsorbents used in this work were exposed to the same conditions used during desorption experiments and were further washed with water to eliminate the SDS or EtOH in excess (blank samples).

The external specific surface area (ESSA) was determined by nitrogen adsorption at 77 K (SN_2) using a Micromeritics model Gemini V, and all samples were dried at 100 °C for 12 h under high vacuum before the nitrogen sorption measurements. The total specific surface area (TSSA) was determined from the adsorption of water vapor at a relative humidity of 0.56, as described elsewhere (Torres Sanchez and Falasca 1997). For OMt samples, water adsorption sites were also determined by same methodology, but due to the hydrophobicity attained (Gamba et al. 2015), this parameter do not indicates accurately the TSSA.

The IEP values of adsorbents were determined by diffusion potential method as described previously (Tschapek et al. 1989).

Zeta potential measurements were carried out with a Zeta Potential Analyzer 90Plus/Bi-MAS (Brookhaven Instruments Corporation), using 10^{-3} M KCl as inert electrolyte and Pd electrodes. Sample suspensions were prepared at several pH values equilibrated for 24 h by dropwise addition of concentrated HCl or KOH solutions.

The particle size determinations was obtained by dynamic light scattering (DLS) measurements using the same Brookhaven equipment (Dapp function) utilized for zeta potential measurements, operating at $\lambda = 635$ nm, 15 mW solid state laser, scattering angle 90°, 25 ± 0.1 °C. All sample suspensions (1% *w/w*) were prepared with water solutions and sonicated for 5 min. The determination rendered the mean apparent equivalent sphere diameter, Dapp. Also polydispersity values were obtained which allowed to indicate the status as nearly monodisperse sample (values from 0.000 to 0.020), narrow distributions (0.020 to 0.080), and larger values for broader distributions.

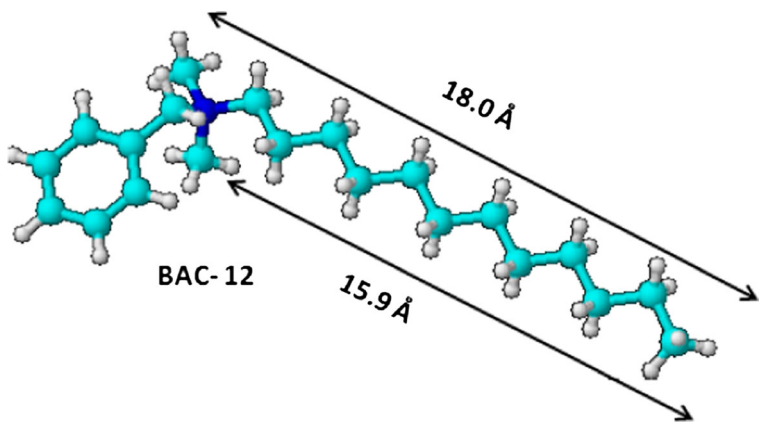

Fig. 2 Molecular structure of BAC-12

Crystallographic data of samples with and without adsorbed BAC were obtained by XRD with a Philips 3710 diffractometer using Cu Kα radiation 40 kV, 20 mA, Ni filter, and patterns collected from 2 to 30° (2θ). The raw Mt, OMt, and BAC adsorbed samples were dried at 60 °C overnight and analyzed as semi-oriented (or powder) samples. Because of the greater precision in d001 value obtained by analysis of oriented samples method (Pacuła et al. 2006), this form of analysis was chosen for a better comparison between XRD diffractograms corresponding to raw Mt, OMt, BAC adsorbed at maximum amount, desorbed with EtOH or SDS, and blank samples. The slide mounts for oriented samples were prepared by drying during 48 h, at room temperature and relative humidity (rh) 0.56, a glass slide covered with the sample slurry.

3 Results and Discussion

3.1 Physicochemical Parameters of Adsorbents

Table 1 resumed characteristic parameters of the different materials. Both raw samples developed different values of the evaluated parameters mainly due to their dissimilar chemical formula as was indicated in Magnoli et al. (2008), which is also reflected in the different IEP values found.

The OMt samples showed a decrease respect to the corresponding raw Mts, of both ESSA (eight and two times for M_{Cas}-C18 and M_{Cloi}-30B, respectively) and TSSA (eight and five times for M_{Cas}-C18 and M_{Cloi}-30B, respectively) values. The close values decrease of both TSSA and ESSA, agree with the 10% corresponding to the edge surface respect to the TSSA surface of montmorillonite (Thomas et al. 1999). The decrease in TSSA values was assigned to diminution of micropore size and surfactant occupancy of the interparticle pores in the OMt samples (Fernández et al. 2014).

Dapp value for both raw Mt was in agreement with that found previously (Fernández et al. 2014), the higher values attained for both raw samples with the respective QAC loaded were assigned to hydrophobic interactions generated by the QAC adsorbed, mainly in the external surface as will be discussed below (zeta potential measurements) and that would affect differently the adsorption/desorption of BAC. The polydispersity values (>0.08) for all samples indicated a broader distributions for all samples evaluated.

In order to understand the evolution of montmorillonite surface charges with the QAC loading, the two different charged sites that coexist on Mt surface must be identified. These surface charges are face or structural (permanent negative) and edge (pH dependent) charges. As micro-electrophoresis measurements use an electric field to determine the surface charge and in montmorillonite there is a higher magnitude of face charges than edge (90 and 10% of the total surface, respectively), IEP value (pH where the overall electric surface charge is neutral) cannot be determined by this technique (Missana and Adel 2000), and an almost constant and negative charge value was attained in a large pH range (Fernández et al. 2013). To take into account all Mt's surface charges, the IEP value must be determined using techniques as potentiometric titrations (Delgado et al. 1986) or by measurements of the diffusion potential method and the IEP obtained were indicated in Table 1. IEP values of raw Mt agree with previously found for other Mt of different provenance (Fernández et al. 2014). The higher IEP pH found for M_{Cloi}-30B with respect to M_{Cloi} (Table 1) was indicative of the importance of QAC surface coverage on M_{Cloi}-30B sample. The presence of the positively charged quaternary ammonium at the surface shifted the IEP pH to a much higher value than that determine for pure M_{Cloi} sample (Bhandarkan et al. 2001).

3.2 BAC Adsorption Experiments and Products Characterization

Figure 3 showed the experimental isotherms of BAC adsorption on all samples with their corresponding Langmuir fit, and Table 2 showed the sorption constants obtained from the linearized form of the Langmuir isotherm. Adsorptions data for raw samples (M_{Cas} and M_{Cloi}) agree with those indicated elsewhere for BAC-12 on Mt (Tahani et al. 1999; Zanini et al. 2013), with a sharp surfactant adsorption increase derived by ion exchange mechanism up to the respective CEC values (0.825 and 0.926 mmol g^{-1}, respectively), and a simultaneous BAC cation-coion (Cl^-) adsorption starting after neutralization of Mt surface charge. Differences of IEP pH value (Table 1) found for both raw samples could also influence the BAC adsorption values obtained, although at the adsorption pH (pH = 6.0) the external surface of both Mt remains negatively charged as it was subsequently evaluated in Fig. 5. For both OMt (M_{Cloi}-30B and M_{Cas}-C18) samples, due to the occupation of

Table 1 Isoelectric point (IEP), external specific surface area (ESSA), total specific surface area (TSSA), apparent diameter (Dapp), and polydispersity

Sample	IEP (pH)	ESSA ($m^2\ g^{-1}$)	TSSA ($m^2\ g^{-1}$)	Dapp (nm)	Polydispersity
M_{Cas}	2.7 ± 0.2	34.00 ± 0.16[a]	621 ± 5[a]	674 ± 51[b]	0.260 ± 0.011
M_{Cloi}	5.0 ± 0.3	19.30 ± 0.12[c]	483 ± 7[c]	504 ± 9	0.214 ± 0.012
M_{Cas}-C18	n.d.	4.14 ± 0.14	74 ± 2	2325 ± 248	0.194 ± 0.045
M_{Cloi}-30B	11.0 ± 0.3	10.00 ± 0.19[c]	91 ± 2[c]	4410 ± 442	0.123 ± 0.047

[a] Data from Bianchi et al. (2013)

[b] Data from Gamba et al. (2015)

[c] Data from Botana et al. (2010)

the adsorption sites by the QACs used to modify each Mt, BAC adsorption values decreased around four times with respect to the corresponding raw Mts, which is not directly related with ratio of TSSA values of the OMts and the respective Mts (OMts/Mt = 8.4 and 5.3, for M_{Cas} and M_{Cloi}, respectively, Table 1) or to the Dapp values which increased 3.4 and 9.6 for M_{Cas} and M_{Cloi}, respectively, with the surfactant loading. BAC adsorption variations between the two OMt could be assigned to the different QAC loading (86 and 100% CEC for M_{Cas}-C18 and M_{Cloi}-30B samples, respectively) and consequently the different BAC interaction with the Mt free surface as discussed below (in the interlayer or inner surface and surface electrical charge or outer surface).

As was identified by Zanini et al. (2013), the best fit of experimental points for BAC adsorption on raw Mt was obtained by using a Langmuir equation with two terms, in agreement to the two different adsorption mechanisms assigned by Tahani et al. (1999). As will be discussed in following paragraphs, in OMts samples BAC adsorption occurred in one step due to the respective QAC partially blockage of the interlayer surface. In order to compare both raw Mt and OMt samples in Table 2, the Langmuir parameters obtained by the linearized model were resumed. The best fit of Langmuir model (R^2) obtained for BAC adsorption by OMts with respect to raw Mt samples reflected the previous indicated adsorption behavior. Also RMSE values, calculated from non-linearized Langmuir model (Tsai and Juang, 2000), indicated similar goodness-of-fit in agreement with R^2.

k_L values are an estimation of the affinity of BAC on the adsorbent surface for M_{Cloi} and M_{Cas} and their respective OMts. The variation of k_L values for M_{Cloi}-30B and M_{Cas}-C18 with respect to the raw Mts points out the different adsorption mechanisms involved in the adsorption process, as indicated previously.

The variation of both Mt surfaces (inner and outer) by BAC adsorption can be followed by analysis of the d001 value by X-ray diffraction [34], which indicates the interlayer (internal surface) modification, and zeta potential value determination which specifies the external electric surface charge variations. The interlayer exchange of raw Mt's inorganic cations (Tahani et al. 1999; Churchman 2002) by different amount or size of organic molecules produces an interlayer expansion and also the water solvation of inorganic cations disappearance. In absence of water, the interlayer space gap for Mt clay was determined from the d001 value and the thickness of a single Mt's tetrahedral-octahedral-tetrahedral (TOT) layer was 0.97 nm (Emmerich et al. 2001). The treatment at 80 °C of raw Mt samples did not allow to attain the thickness of a single Mt's TOT layer; however, similar d001 values of 1.02 and 1.09 nm between M_{Cas} and M_{Cloi} samples (Fig. 4) were found, which are closer to that of single Mt's TOT layer.

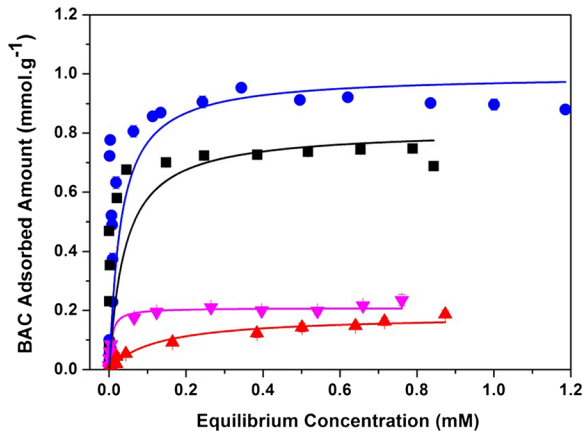

Fig. 3 Adsorption isotherms of BAC, at pH 6, on (*black square*) M_{Cas}, (*blue circle*) M_{Cloi}, (*pink inverted triangle*) M_{Cloi}-30B, and (*red triangle*) M_{Cas}-C18 samples. *Solid lines* indicated Langmuir fit

Table 2 Parameters from the linearized form of the Langmuir model fitted to the experimental adsorption data

Sample	Q_{max} (mmol g^{-1})	k_L (L $mmol^{-1}$)	R^2	RMSE[a]
M_{Cloi}	0.93 ± 0.02	33 ± 12	0.9862	0.235
M_{Cas}	0.74 ± 0.02	51 ± 12	0.9876	0.190
M_{Cloi}-30B	0.22 ± 0.01	70 ± 20	0.9912	0.013
M_{Cas}-C18	0.19 ± 0.01	8 ± 2	0.9908	0.014

[a] RMSE was calculated from non-linearized Langmuir model (Tsai and Juang 2000)

The increase of BAC adsorption on M_{Cas} and M_{Cloi} samples generated a shift of d001 value in two steps. For BAC adsorbed amount <0.5 mmol g^{-1}, a first 001 reflection shift occurred from around 1.00 nm to around 1.49 nm, while for higher BAC adsorbed amount, a second shift was evidenced from 1.49 to 1.75 nm (Fig. 4). These interlayer gaps allowed the entrance of BAC from sideway or parallel (see Fig. 2) to the basal space in a monolayer arrangement in agreement with data found by Tahani et al. (1999) for BAC adsorption <0.8 CEC (or BAC adsorbed amount 0.75 mmol g^{-1}).

For M_{Cas}-C18 and M_{Cloi}-30B samples, a lower 001 reflection shift of 0.15 and 0.05 nm (Fig. 4), respectively, was found after BAC adsorption, which indicated a rearrangement of the respective surfactants in the interlayer.

The ζ curves as a function of pH (Fig. 5) were determined for all adsorbents and products with two different BAC amount adsorbed (attained with $C_0 = 0.01$ mM and the maximal amount obtained in Fig. 3).

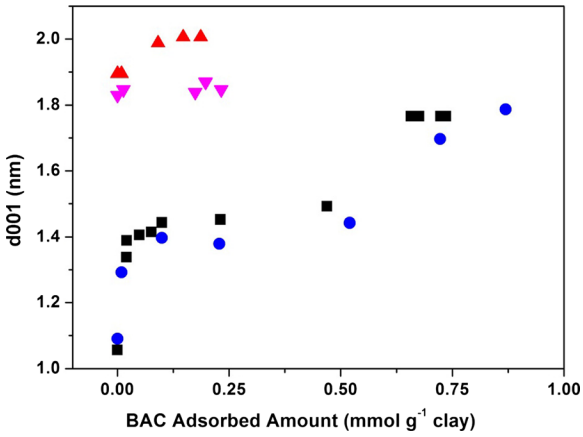

Fig. 4 Basal plane distances for semi-oriented samples with increasing BAC adsorbed amount . symbols indicated (*blue circle*) M_{Cloi}, (*black square*) M_{Cas}, (*pink inverted triangle*) M_{Cloi}-M30B, and (*red triangle*) M_{Cas}-C18 samples

In order to understand the ζ value obtained for Mt samples, and as was showed by Pecini and Avena (2013), the permanent charges (at the inner or interlayer surface) in raw Mt and in OMt samples remained neutralized by the presence of raw inorganic or organic (surfactant or QAC) exchanged cations, and are not evaluated by micro-electrophoresis method. Resuming, this method allows to mainly evaluate the charge changes in the particles external face and edge (outer surface) which correspond to 10% of the total surface, attaining at ζ = 0 the pH of IEP_{edge} (Pecini and Avena 2013). The edge surface is pH dependent (Churchman 2002) and the different arrangement of the organic molecules involved on this surface (BAC on raw Mts or BAC and the respective surfactants on OMts samples) generated the change of electric charges found (Fig. 5a, b).

It is important to highlight that while the ζ curve indicated that external surfaces of both raw Mt remained negatively charged throughout the pH range evaluated (Fig. 5a, b) (Lombardi et al. 2006) particularly at pH = 6, their ζ values were very close (−35 and −36 mV for M_{Cas} and M_{Cloi} samples, respectively), and consequently the differences of BAC adsorption found (Table 1) cannot be assigned only to its interaction with the external surface sites. These results indicated that differences between the CEC or IEP pH values for M_{Cas} and M_{Cloi} (Table 1), respectively, appear to have greater importance in the BAC adsorption capacity of these samples.

The presence of surfactant on each OMt generated different electrical surface charge behavior within these samples. For M_{Cas}-C18 sample, a decrease of negative charge with respect to M_{Cas} sample was found, while for M_{Cloi}-30B sample a reversion to positive surface charge up to pH 5.5 (pH of the IEP_{edge}) with respect to M_{Cloi} sample was found. This different surface charge behavior was assigned to the different QAC loading (0.86 and 1.0 CEC for M_{Cas}-C18 and M_{Cloi}-30B samples, respectively) and also to the different QAC used to attain the OMt samples (Bianchi et al. 2013).

Mts and OMts with adsorbed BAC displayed different mobility behavior depending on the amount of BAC adsorbed and also between samples (Fig. 5a, b). For raw Mts, samples with low amount of adsorbed BAC showed no change of ζ values with respect to same samples without adsorbed BAC. However, a huge decrease of negative charge was produced when maximal BAC adsorption was attained (Fig. 5a, b and Fig. 8). In the case of OMt samples (Fig. 8), increase of BAC

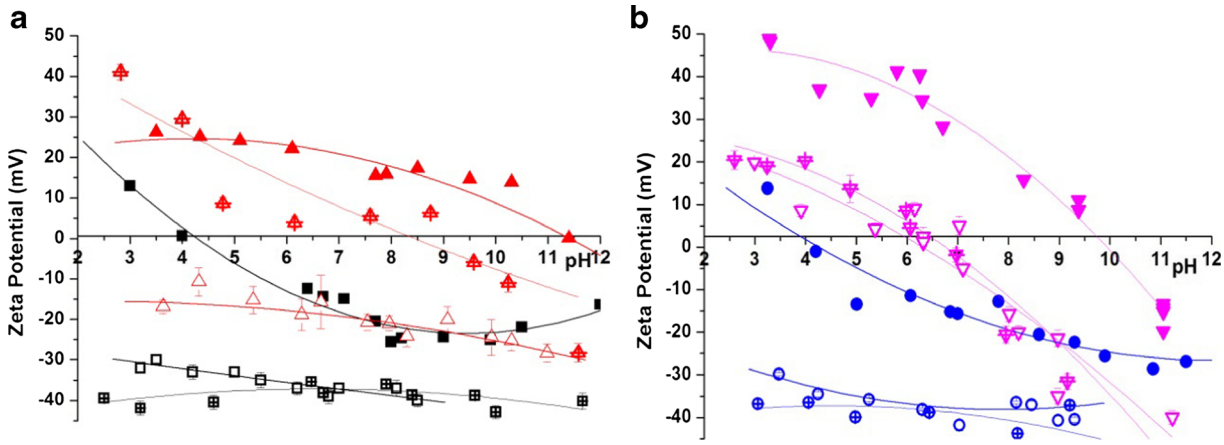

Fig. 5 Zeta potential curves for **a** M_{Cas} and M_{Cas}-C18 and **b** M_{Cloi} and M_{Cloi}-30B. Symbol indicated (*blue circle*) M_{Cloi}, (*black square*) M_{Cas}, (*red triangle*) M_{Cas}-C18, and (*pink inverted triangle*) M_{Cloi}-30B samples. Symbols: (*empty*) samples without BAC; (*empty with cross*) $C_0 = 0.01$ mM, and (*full*) samples with BAC maximal adsorption

adsorption generated a different but correlated increase of the positive ζ value.

The behavior presented by raw Mt samples indicated, in agreement with that found for benzimidazole (Torres Sánchez et al. 2011), that BAC concentration threshold necessary to start the outer surface coating was not yet reached at $C_0 = 0.01$ mM, while the BAC entrance at the interlayer was yet attained (Fig. 4). In the case of OMt samples, for low concentration of adsorbed BAC, some arrangement of BAC and surfactant on the outer surface generated an increase of the positive charge with respect to same samples without BAC. Particularly at pH = 6 (pH of the BAC adsorption evaluation), the ζ values changed from −15 to 5 and from 5 to 10 mV values for BAC-M_{Cas}-C18 and BAC-M_{Cloi}-30B samples, respectively.

The adsorption of the maximum amount of BAC on all samples at pH = 6 (Fig. 3), due to the BAC positive charge (which is independent of the pH), generated a decrease of negative surface charge on raw Mt samples (Fig. 5a, b), while an important increase of positive ζ value was found for BAC-M_{Cas}-C18 and BAC-M_{Cloi}-30B samples.

It is important to note that for raw Mt samples (BAC-M_{Cas} and BAC-M_{Cloi}), same IEP_{edge} (ζ = 0) at pH ≈ 4.0 was attained due to the similar concentration of BAC adsorbed (Fig. 3 and Table 2), which was enough to cover the solid surface (Lombardi et al. 2006). For OMt samples, the different maximum amount of BAC adsorbed and QAC used to obtain OMt produced a different increase of the positive surface charge found (Fig. 5a, b), attaining the IEP_{edge} at pH around 10 for both samples.

Same behaviors can be extracted by examining the difference produced in the external surface charge by the BAC adsorption, at pH = 6, analyzing two samples of each adsorbent with BAC adsorbed at initial concentrations $C_0 = 0.01$ mM and C_0 = maximum adsorption. These BAC adsorptions corresponded to 0.79; 0.92, 0.13, and 0.24 mmol g^{-1} BAC for M_{Cas}, M_{Cloi}, M_{Cas}-C18, and M_{Cloi}-30B samples, respectively (Fig. S1 in supplementary information). For samples M_{Cas}-C18 and M_{Cloi}-30B, the respective neutral and negative surface charged were modified to positive surface charged (3.96 and 7 mV, respectively). For maximum BAC adsorption 0.79 and 0.92 mmol g^{-1} for M_{Cas} and M_{Cloi} samples, respectively, a close decrease of negative charge of around −12 mV was found, whereas for M_{Cas}-C18 and M_{Cloi}-30B samples, the BAC adsorption of 0.13 and 0.24 mmol g^{-1} resulted in an increase of 18.24 and 36.1 mV of the positive surface charge, respectively. It was interesting to note that for M_{Cas}-C18 and M_{Cloi}-30B samples, whose external surface was covered by the surfactant, the subsequent adsorption of BAC generated an increase of positive charge proportional to the BAC amount adsorbed, independently of the surfactant used.

3.3 Desorption Experiments

The amount of BAC adsorbed on the samples used in the desorption process was that of maximal adsorption for each adsorbent. The amount of BAC released to the solution indicated the fraction of BAC desorbed from the material with respect to the initial amount of BAC contained in the evaluated adsorbent. It should be

noticed that the initial amount of BAC was different among the studied adsorbent as it is indicated in Fig. 6, where the BAC desorption (in mmol g^{-1} units) attained with respect to the corresponding sample with BAC adsorption obtained at pH = 6.0 (20 mg/20 mL dispersions) for all samples and solvents used is shown. The amount of BAC adsorbed and desorbed by percentage of material was indicated in Supporting Information (Table S1).

The BAC desorption in hot water was negligible, and because of this it is not indicated in Fig. 6, while when the medium pH was changed from acid to alkaline a low but opposite desorption behavior appeared within Mt or OMt samples studied. For raw Mts, although the BAC adsorption mechanism is mainly ion exchange (Tahani et al. 1999; Zanini et al. 2013), certain electrostatic interaction may occurred, generating a significative BAC desorption values in acidic medium (pH = 3) with respect to those achieved in alkaline medium. This behavior can be assigned to the almost neutral surface charge of both raw samples in acid medium, as indicated by their IEP pH (Table 1), while in alkaline medium (pH = 11) the negative surface charge attained for both Mts could influence the decrease of BAC desorption values. The lower values of BAC desorption attained for OMt in aqueous medium (acid or alkaline, Fig. 6) could be assigned to the lower negative surface charge of these samples with respect to the raw Mts, as will be discussed in further section (zeta potential analysis).

BAC desorption values increased significantly for all samples in EtOH and even more in SDS medium, with respect to water medium, and would be related to different surface effect of both solvents that will be evaluated by XRD and ζ analysis in next paragraphs.

3.4 X-Ray Diffraction Analysis of BAC Desorbed Samples

Due to the low amount of BAC desorbed in acid and alkaline media, differences of d001 values of the BAC desorbed respect to that with BAC adsorbed samples will be out of the XRD detection limit (2%) and were not analyzed.

Before to analyze the BAC desorbed samples in SDS and EtOH media, the effect of both solvents on the interlayer of all samples (without BAC) was studied. In order to obtain a higher accuracy in the d001 values generated, all samples were analyzed in oriented form (Pacuła et al. 2006) (Fig. 7a, b). It should be noted that while for OMt samples no difference between the d001 values was found (Fig. 4 and Fig. 7a) in agreement with was indicated by Zhu et al. (2011), for raw Mt samples a d001 value increase of approximately 0.2 nm can be observed and assigned to the hydration of inorganic cations (Ferrage et al. 2005) by the oriented method.

Mt and OMt samples treated with EtOH (Fig. 7a) showed a d001 value increase of around 0.2 and 0.1 nm, respectively, in agreement with data found by Mozorov et al. (2014).

The SDS treatment generated a close d001 value for all samples (without BAC adsorbed) at around 1.5 nm (Fig. 7a). The difference in d001 value of around 0.2 nm

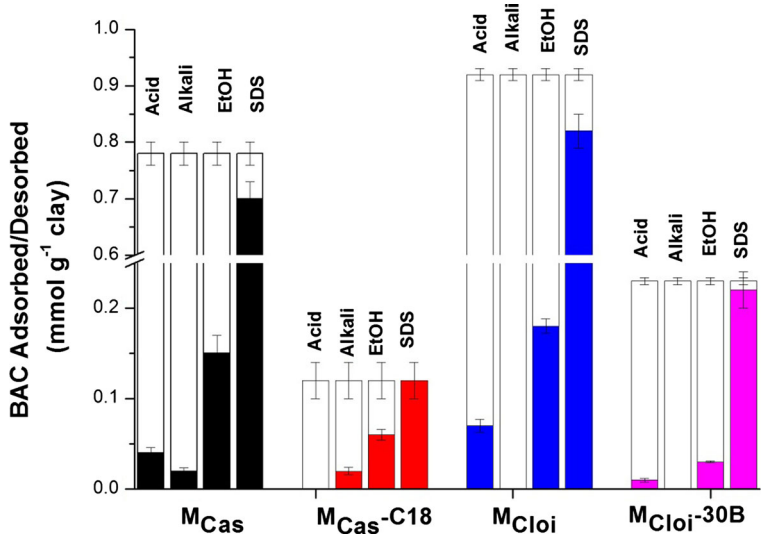

Fig. 6 BAC adsorbed (*empty bar*) and desorbed (*full bar*) for the indicated samples and media

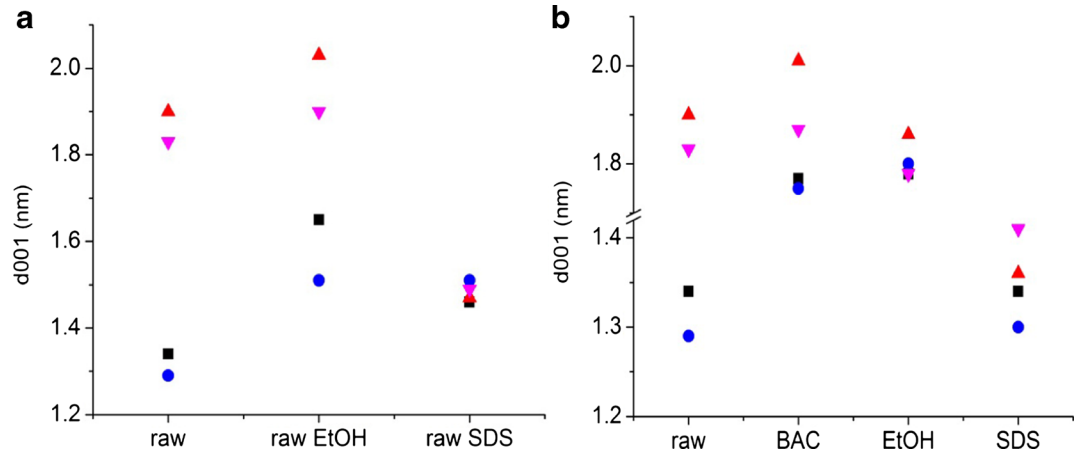

Fig. 7 d001 values for oriented samples: **a** without BAC; **b** with max. BAC adsorbed (*BAC*) and further desorption in EtOH or SDS. Raw samples were added in order to compare the 001 reflections changes. Symbols indicated (*red circle*) M_{Cloi}, (*black square*) M_{Cas}, (*pink inverted triangle*) M_{Cloi}-M30B, and (*red triangle*) M_{Cas}-C18 samples. *Solid lines* are a guide for the eye

between raw Mt and SDS treated samples might indicate the SDS entrance in the interlayer. The high concentration of SDS used (5% *w*/*v*, corresponding to 210 times the CEC of both Mt) can generate the difference with respect to the behavior found by Zhang et al. (2010) who indicated null interlayer insertion of the SDS anion when three times the CEC concentration was used.

Particularly, for OMt samples, the SDS medium (Fig. 7a) produced a huge decrease of d001 value (of around 0.50 nm) that due to the high surfactant loading cannot be assigned to dehydration of OMt samples (Zhu et al. 2011) and consequently indicated an important desorption of the respective initial surfactant.

Raw Mt samples with maximum amount of adsorbed BAC (BACmax) and further desorption in EtOH medium showed a small interlayer increase (of around 0.1 nm) with respect to the corresponding samples with adsorbed BAC (Fig. 7b). Due to the increase of d001 values found for Mt samples (without BAC) in the presence of EtOH (Fig. 7a), and the important amount of BAC desorbed in this medium (Fig. 6), the interlayer increase could be assigned to a compensation between both behaviors.

Similar trend was found for OMt samples with BAC desorbed in EtOH. The interlayer shrinkages found were 0.2 and 0.1 nm (for M_{Cas}-C18 and M_{Cloi}-M30B samples, respectively) with respect to the same samples with adsorbed BAC, and attained slightly lower d001 values with respect to those of initial OMt samples.

For all samples, the opposite behaviors generated by EtOH alone (increase of interlayer, Fig. 7a), and for BAC adsorption and further desorption in EtOH medium (decrease of interlayer, Fig. 7b), do not allow to identify whether BAC only (as shown Fig. 4) or surfactant + BAC was desorbed from the interlayer.

When BACmax adsorbed samples with subsequent SDS treatment were analyzed (Fig. 7b), a decrease of d001 values ranging from 0.65 to 0.44 nm was found with respect to same samples with BAC adsorbed. The close d001 values obtained for raw Mt and Mt treated with BAC and further SDS samples indicated the interlayer desorption of BAC (Fig. 4). While for BAC-M_{Cas}-C18 and BAC-M_{Cloi}-M30B samples the interlayer shrinkage (0.65 and 0.46 nm, respectively) produced after SDS treatment approached the d001 values obtained for raw Mt, which indicated the release of BAC and also the respective QAC (in agreement to that observed for OMt samples without BAC in SDS media, Fig. 7a).

3.5 Zeta Potential Measurements of BAC Desorbed Samples

As was performed for XRD analysis, the effect of both solvents (EtOH and SDS) on the electric external surface charge of all samples (without BAC) was studied, at pH = 6, and indicated in Fig. 8a. No effect of EtOH nor SDS was found on external surface change of both raw Mt, contrarily to that found for OMt samples where an increase of negative surface, more pronounced for SDS than EtOH solvent, was found. These results, indicating different desorption of the surfactant coating from the external surface of the OMt samples, besides to that

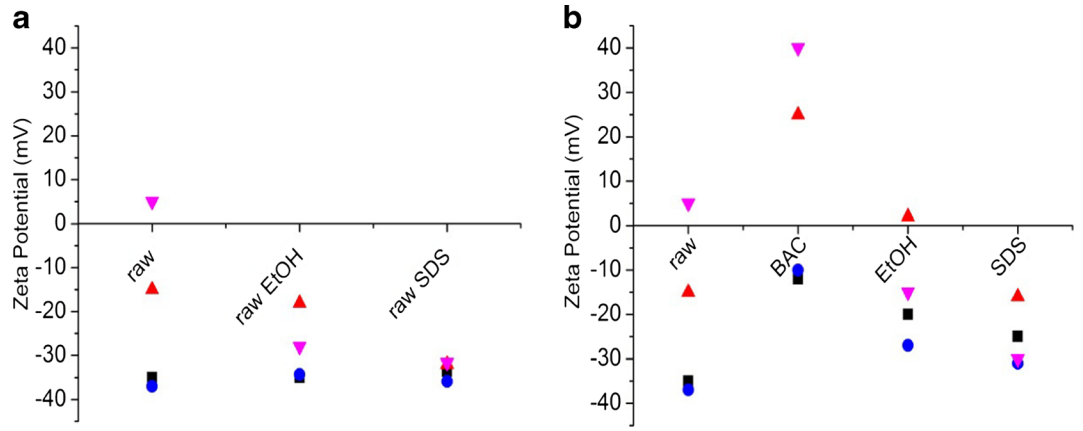

Fig. 8 Zeta potential values, at pH 6 for: **a** without BAC; **b** with BACmax adsorbed and further desorption in EtOH or SDS. Raw samples were added in order to compare the zeta potential values. Symbols indicated (*blue circle*) M_{Cloi}, (*black square*) M_{Cas}, (*red triangle*) M_{Cas}-C18, and (*pink inverted triangle*) M_{Cloi}-30B samples

desorbed from the interface indicated by XRD. Particularly, for SDS solvent similar, both OMt samples attained values of negative external surface charges close to those of the original raw Mt samples.

Desorption of BAC on raw Mt (evaluated on BACmax samples, zeta potential curves Fig S2 and S3 in Supporting Information), at pH = 6, in EtOH medium increased the negative zeta potential value with respect to those of respective samples with maximal BAC adsorption, without attaining the zeta potential value of raw samples, which indicated a partial disappearance of BAC from the outer surface (Fig. 8b). Similar and more pronounced trend on zeta potential values produced the SDS medium for BAC desorption on raw Mt samples.

For OMt samples, the BAC desorption in both EtOH and SDS media (zeta potential curves Fig S4 and S5 in Supporting Information) produced an important, but different, decrease of the positive zeta potential values with respect to those attained previously with the BAC adsorption.

For BAC-M_{Cas}-C18 sample, the BAC desorption in EtOH medium attained similar zeta potential value, at pH 6, than that obtained with low BAC adsorption (5 mV, Fig. 5a). Taking into account that the interlayer variations (Fig. 7a, b) did not allow to identify whether BAC alone or with surfactant was desorbed, the 44% desorption (Table S1 in Supporting Information) would be mainly coming from the outer surface. While BAC-M_{Cas}-C18 sample in SDS medium attained a zeta potential value close to that of M_{Cas}-C18 sample, indicating that almost all BAC was desorbed and the QAC remained at the outer surface (Fig. 8b), while BAC and QAC were desorbed from the interlayer (Fig. 7b), in agreement with the huge BAC desorption (Fig. 6 or 99% desorption indicated in Table S1 in Supporting Information).

For BAC-M_{Cloi}-30B sample, the BAC desorption in EtOH medium decrease the positive zeta potential value with respect to that attained with the BAC adsorption, and also to lower value than that of the M_{Cloi}-30B sample. This behavior indicated the partial disappearance of BAC (13% desorption indicated in Table S1 in Supporting Information) and mainly the QAC of the outer surface, while in the interlayer, some BAC due to the higher d001 value with respect to the raw Mt could remain (Fig. 7b). The BAC desorption in SDS medium produced a more pronounced decrease of zeta potential value (91% desorption indicated in Table S1 in Supporting Information) than that originated by EtOH medium and also the interlayer was collapsed to values of the raw Mt, both behavior indicated a complete BAC and surfactant loss from the solid.

4 Conclusions

The BAC adsorption on raw Mts attained a maximum amount equivalent to the respective CEC, occurred in two steps related with the BAC concentration, and involved differently the outer surface and the interlayer space. During the first step, with BAC concentration adsorbed amount <0.5 mmol g^{-1} (or < 0.8 CEC), an interlayer expansion of 0.49 nm indicated the BAC entrance, while the constant Mt's negative surface charge indicated no interaction with the outer surface.

The second adsorption step, for BAC concentration adsorbed amount >0.5 mmol g^{-1}, generated a new interlayer expansion of around 0.26 nm (allowing the BAC entrance in a monolayer arrangement, from sideway or parallel to the basal space), exceeding the threshold concentration for developing electrostatic adsorption mechanisms on the outer surface. The latter behavior was evidenced by the reversal from negative to positive surface electric charge, attaining an IEP_{edge} for both Mt at pH = 4.0.

The QAC surface occupancy on OMts generated a decrease of four times the BAC adsorption with respect to the correspondent value attained for raw Mt samples. A slight increase of d001 values with BAC adsorption indicated a rearrangement of the respective QACs with the BAC presence in the interlayer, while the outer surface pointed out a continuous increase of positive surface charge with the further BAC loading.

These different BAC adsorption mechanism in Mt and OMt samples produced lower relative desorption in aqueous medium (acid or alkaline) for OMt than Mt samples, while both EtOH and SDS media increased the BAC desorption in different amount for all samples.

For raw Mts, the low increase of d001 value with EtOH medium cannot allow to identify the BAC removal from the interlayer, while decrease of zeta potential negative value indicated an important amount of BAC release (40%) from the outer surface. For these samples, the SDS medium removed almost all BAC (88%) from the interlayer while the fact that the zeta potential negative value did not reach that of raw samples without BAC indicated that some BAC remain in the outer surface.

For OMts samples, the BAC desorption in EtOH medium indicated different behaviors linked to the existence of different QACs in both samples. For BAC-M_{Cas}-C18 sample, the interlayer changes failed to identify if only BAC or also QAC were partially desorbed, as in the outer surface. The presence of SDS generated a complete BAC and QAC desorption from the interlayer, while remained at the outer surface.

For sample BAC-M_{Cloi}-30B in EtOH medium, followed similar trend than that of BAC-M_{Cas}-C18 sample, the changes of d001 value found cannot recognize if only BAC or also the QAC were partially desorbed, while both disappeared largely from the external surface. In SDS medium, desorption of BAC and QAC in BAC-M_{Cloi}-30B was not as complete as in BAC-M_{CAS}-C18 sample, while both were complete loss from the outer surface.

Based on these results, it was inferred that BAC adsorbed on Mt or OMt in aqueous media enabled its use in technological applications friendly to the environment.

Acknowledgments The authors acknowledge the funding provided by FONARSEC project, Nano FS-008/2010 and ANPCyT-PICT 2014/585 and PICT 2014 2386. RC and RMTS are members of CONICET and FY acknowledges CIC Prov. Bs. As., and ELL and FMF the CONICET for their respective fellowships.

References

Bellotti, N., Romagnoli, R., Quintero, C., Domínguez-Wong, C., Ruiz, F., & Deyá, C. (2015). Nanoparticles as antifungal additives for indoor water borne. *Progress in Organic Coatings, 86*, 33–40.

Bhandarkan, S. D., Gardner, D., Chandross, E. A., Hill, M., Putvmskl, T. M., Plams, S. (2001). Method for forming article using sol-gel processing. US 6,209,357 B1.

Bianchi, A. E., Fernández, M., Pantanetti, M. R., Viña, I., Torriani, I., Torres Sánchez, R. M., & Punte, G. (2013). $ODTMA^+$ and $HDTMA^+$ organo-montmorillonites characterization: new insight by WAXS, SAXS and surface charge. *Applied Clay Science, 83–84*, 280–285.

Botana, A., Mollo, M., Eisenberg, P., & Torres Sánchez, R. M. (2010). Effect of modified montmorillonite on biodegradable PHB nanocomposites. *Applied Clay Science, 47*, 263–270.

Buser, A. M., & Morf, L. S. (2009). Substance flow analysis of quaternary ammonium compounds for Switzerland, modelling the consumption in biocidal applications and emissions to the environment. *Umweltwissenschaften und Schadstoff-Forschung, 21*(1), 27–35.

Churchman, G. J. (2002). Formation of complexes between bentonite and different cationic polyelectrolytes and their use as sorbents for non-ionic and anionic pollutants. *Applied Clay Science, 21*, 177–189.

Delgado, A., Gonzalez-Caballero, F., & Bruque, J. M. (1986). On the zeta potential and surface charge density of montmorillonite in aqueous electrolyte solutions. *Journal of Colloid and Interface Science, 113*, 203–211.

Emmerich, K., Plötze, M., & Kahr, G. (2001). Reversible collapse and Mg^{2+} release of de- and re-hydroxylated homoionic cis-vacant montmorillonites. *Applied Clay Science, 19*, 143–154.

EPA, Environmental Protection Agency (2006). Prevention, pesticides and toxic substances (7510C). EPA739-R-06e009.

Fernández, M., Alba, M. D., Torres Sánchez, R. M. (2013). Thermal or mechanical treatments effects on mono and polyvalent cations homoionized MMt: an insight of the surface and structural changes. Colloids and Surfaces, A, 423, 1-10.

Fernández, M., Curutchet, G., & Torres Sánchez, R. M. (2014). Removal of humic acid by organo-montmorillonites: influence of surfactant loading and chain length of alkylammonium cations. *Water, Air, & Soil Pollution, 225*(6), 1–11.

Ferrage, E., Lanson, B., Sakharov, B. A., & Drits, V. A. (2005). Investigation of smectite hydration properties by modeling

experimental X-ray diffraction patterns: part I. Montmorillonite hydration properties. *American Mineralogist, 90*(8-9), 1358–1374.

Ferrer, I., & Furlong, E. (2001). Identification of alkyl dimethylbenzylammonium surfactants in water samples by solid-phase extraction followed by ion trap LC/MS and LC/MS/MS. *Environmental Science and Technology, 35*, 2583–2588.

Gamba, M., Flores, F. M., Madejová, J., & Torres Sánchez, R. M. (2015). Comparison of imazalil removal onto montmorillonite and nanomontmorillonite and adsorption surface sites involved: an approach for agricultural wastewater treatment. *Industrial & Engineering Chemistry Research, 54*(5), 1529–1538.

Gast, R. G., & Mortland, M. M. (1971). Self diffusion of alkylammonium ions in montmorillonite. *Journal of Colloid and Interface Science, 37*, 80–92.

Gromaire, M. C., Van de Voorde, A., Lorgeoux, C., & Chebbo, G. (2015). Roof maintenance practices, benzalkonium runoff from roofs treated with biocide products in situ pilot-scale study. *Water Research, 81*, 279–287.

Hoque, J., Akkapeddi, P., Yadav, V., Manjunath, G. B., Uppu, D. S. S. M., Konai, M. M., Yarlagadda, V., Sanyal, K., & Haldar, J. (2015). Broad spectrum antibacterial and antifungal polymeric paint materials: synthesis, structure–activity relationship, and membrane-active mode of action. *Applied Materials & Interfaces, 7*, 1804–1815.

Jones, T. R. (1983). The properties and uses of clays which swell in organic solvents. *Clay Minerals, 18*, 399–410.

Khalil, R. K. S. (2013). Selective removal and inactivation of bacteria by nanoparticle composites prepared by surface modification of montmorillonite with quaternary ammonium compounds. *World Journal of Microbiology and Biotechnology, 29*, 1839–1850.

Khan, A. M., & Shah, S. S. (2008). CMC of sodium dodecyl sulfate and the effect of low concentration of pyrene on its CMC using ORIGIN software. *Journal of the Chemical Society of Pakistan, 30*(2), 186–191.

Krishnamoorthy, K., Premanathan, M., Veerapandian, M., & Kim, S. J. (2014). Nanostructured molybdenum oxide-based antibacterial paint: effective growth inhibition of various pathogenic bacteria. *Nanotechnology, 25*, 315101.

Kwolek, T., Hodorowicz, M., Stadnicka, K., & Czapkiewicz, J. (2003). Adsorption isotherms of homologous alkyldimethylbenzylammonium bromides on sodium montmorillonite. *Journal of Colloid and Interface Science, 264*, 14–19.

Lagaly, G., Ogawa, M., & Dékány, I. (2006). Clay mineral organic interactions. In F. Bergaya & G. Lagaly (Eds.), *Handbook of clay science* (pp. 309–377). Amsterdam: Elsevier.

Lombardi, B., Torres Sánchez, R. M., Eloy, P., & Genet, M. (2006). Interaction of thiabendazole and benzimidazole with montmorillonite. *Applied Clay Science, 33*, 59–65.

Magnoli, A. P., Tallone, L., Rosa, C. A. R., Dalcero, A. M., Chiacchiera, S. M., & Torres Sánchez, R. M. (2008). Commercial bentonites as detoxifier of broiler feed contaminated with aflatoxin. *Applied Clay Science, 40*, 63–71.

Missana, T., & Adel, A. (2000). On the applicability of DLVO theory to the prediction of clay colloids stability. *Journal of Colloid and Interface Science, 230*, 150–156.

Mozorov, G., Breus, V., Nekludov, S., & Breust, I. (2014). Sorption of volatile organic compounds and their mixtures on montmorillonite at different humidity. *Colloids and Surfaces, A, 454*, 159–171.

Mukherjee, K., Rivera, J. J., & Klibanov, A. M. (2008). Practical aspects of hydrophobic polycationic bactericidal "paints". *Applied Biochemistry and Biotechnology, 151*, 61–70.

Özdemir, G., Yapar, S., & Limoncu, M. (2013). Preparation of CP-Mt for antibacterial applications. *Applied Clay Science, 72*, 201–205.

Pacuła, A., Bielańska, E., Gaweł, A., Bahranowski, K., & Serwicka, E. M. (2006). Textural effects in powdered montmorillonite induced by freeze-drying and ultrasound pretreatment. *Applied Clay Science, 32*, 64–72.

Pecini, E. M., & Avena, M. J. (2013). Measuring the isoelectric point of the edges of clay mineral particles: the case of montmorillonite. *Langmuir, 29*, 14926–14934.

Pérez, P., Fernández, E., & Beiras, R. (2009). Toxicity of benzalkonium chloride on monoalgal cultures and natural assemblages of marine phytoplankton. *Water Air Soil Pollution, 201*, 319–330.

Rosen, M. J. (1989). *Surfactants and interfacial phenom* (2nd ed.). N.York: Wiley.

Savas, L. A., & Hancer, M. (2015). Montmorillonite reinforced polymer nanocomposite antibacterial film. *Applied Clay Science, 108*, 40–44.

Sheng, G., Xu, S., & Boyd, S. A. (1996). Mechanism controlling sorption of neutral organic contaminants by surfactant-derived and natural organic matter. *Environmental Science & Technology, 30*(5), 1553–1557.

Tahani, A., Karroua, M., Van Damme, H., Levitz, P., & Bergaya, F. (1999). Adsorption of a cationic surfactant on Na-montmorillonite: Inspection of adsorption layer by X-ray and fluorescence spectroscopies. *Journal of Colloid and Interface Science, 216*, 242–249.

Thomas, F., Michot, L. J., Vantelon, D., Montargès, E., Prélot, E. B., & Cruchaudet, M. (1999). Layer charge and electrophoretic mobility of smectites. *Colloids and Surfaces, A, 159*, 351–358.

Torres Sánchez, R. M., Genet, M. J., Gaigneaux, E. M., dos Santos Afonso, M., & Yunes, S. (2011). Benzimidazole adsorption on the external and interlayer surfaces of raw and treated montmorillonite. *Applied Clay Science, 53*, 366–373.

Torres Sanchez, R. M., & Falasca, S. (1997). Specific surface and surface charges of some Argentinian soils. *Zeitschrift für Pflanzenernährung und Bodenkunde, 160*, 223–226.

Tsai, S. C., & Juang, K. W. (2000). Comparison of linear and non-linear forms of isotherm models for strontium sorption on a sodium bentonite. *Journal of Radioanalytical Nuclear Chemistry, 243*, 741–746.

Tschapek, M., Torres Sánchez, R. M., & Wasowski, C. (1989). Handy methods for determining the isoelectric point of soils. *Zeitschrift für Pflanzenernährung und Bodenkunde, 152*, 73–76.

Walker, J. R. L., & Evans, S. (1978). Effect of quaternary ammonium compounds on some aquatic plants. *Marine Pollution Bulletin, 9*, 136–137.

Xu, H., Wan, Y., Li, H., Zheng, S., & Zhu, D. (2011). Sorption of aromatic ionizable organic compounds to montmorillonites modified by hexadecyltrimethyl ammonium and polydiallyldimethyl ammonium. *Journal of Environmental Quality, 40*(6), 1895–1902.

Zanini, G. P., Ovesen, R. G., Hansen, H. C. B., & Strobel, B. W. (2013). Adsorption of the disinfectant benzalkonium chloride on montmorillonite. Synergistic effect in mixture of molecules with different chain lengths. *Journal of Environmental Management, 128*, 100–105.

Zhang, C., Cui, F., Zeng, G.-M., Jiang, M., Yang, Z.-Z., Yu, Z.-G., Zhu, M.-Y., & Shen, L.-G. (2015). Quaternary ammonium compounds (QACs): a review on occurrence, fate and toxicity in the environment. *Science of the Total Environment, 518–519*, 352–362.

Zhang, Z., Liao, L., & Xia, Z. (2010). Ultrasound-assisted preparation and characterization of anionic surfactant modified montmorillonites. *Applied Clay Science, 50*, 576–581.

Zhu, J., Wang, T., Zhu, R., Ge, F., Yuan, P., & He, H. (2011). Expansion characteristics of organo montmorillonites during the intercalation, aging, drying and rehydration processes: effect of surfactant/CEC ratio. *Colloids and Surfaces, A, 384*, 401–407.